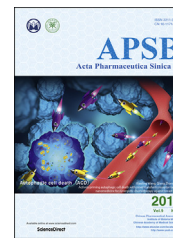




Chinese Pharmaceutical Association  
Institute of Materia Medica, Chinese Academy of Medical Sciences

Acta Pharmaceutica Sinica B

[www.elsevier.com/locate/apsb](http://www.elsevier.com/locate/apsb)  
[www.sciencedirect.com](http://www.sciencedirect.com)



# Kinsenoside attenuates osteoarthritis by repolarizing macrophages through inactivating NF- $\kappa$ B/MAPK signaling and protecting chondrocytes

Feng Zhou<sup>†</sup>, Jingtian Mei<sup>†</sup>, Xiuguo Han, Hanjun Li, Shengbing Yang, Minqi Wang, Linyang Chu, Han Qiao<sup>\*</sup>, Tingting Tang<sup>\*</sup>

Shanghai Key Laboratory of Orthopaedic Implants, Department of Orthopaedic Surgery, Shanghai Ninth People's Hospital, Shanghai Jiao Tong University School of Medicine, Shanghai 200011, China

Received 7 November 2018; received in revised form 14 November 2018; accepted 28 January 2019

## KEY WORDS

Kinsenoside;  
Osteoarthritis;  
Macrophages;  
Polarization;  
Chondrocytes

**Abstract** The objective was to investigate the effect of kinsenoside (Kin) treatments on macrophage polarity and evaluate the resulting protection of chondrocytes to attenuate osteoarthritis (OA) progression. RAW264.7 macrophages were polarized to M1/M2 subtypes then administered with different concentrations of Kin. The polarization transitions were evaluated with quantitative real-time polymerase chain reaction (qRT-PCR), confocal observation and flow cytometry analysis. The mechanism of Kin repolarizing M1 macrophages was evaluated by Western blot. Further, macrophage conditioned medium (CM) and IL-1 $\beta$  were administered to chondrocytes. Micro-CT scanning and histological observations were conducted *in vivo* on anterior cruciate ligament transection (ACLT) mice with or without Kin treatment. We found that Kin repolarized M1 macrophages to the M2 phenotype. Mechanistically, Kin inhibited the phosphorylation of I $\kappa$ B $\alpha$ , which further reduced the downstream phosphorylation of P65 in nuclear factor- $\kappa$ B (NF- $\kappa$ B) signaling. Moreover, Kin inhibited mitogen-activated protein kinases (MAPK) signaling molecules p-JNK, p-ERK and p-P38. Additionally, Kin attenuated macrophage CM and IL-1 $\beta$ -induced chondrocyte damage. *In vivo*, Kin reduced the infiltration of M1 macrophages,

**Abbreviations:** AP-1, activator protein-1; Arg-1, arginase-1; BV, bone volume; BV/TV, bone volume/total tissue volume; C/EBP  $\beta$ , CCAAT/enhancer-binding protein  $\beta$ ; CM, conditioned medium; DMEM, Dulbecco's minimum essential medium; GA, gouty arthritis; H&E, hematoxylin & eosin; HUVECs, human umbilical vein endothelial cells; IFN- $\gamma$ , interferon- $\gamma$ ; iNOS, inducible nitric oxide synthase; IRF4, interferon regulatory factor 4; Kin, kinsenoside; LPS, lipopolysaccharides; MAPK, mitogen-activated protein kinases; MSU, monosodium urate; NF- $\kappa$ B, nuclear factor- $\kappa$ B; NSAIDs, non-steroidal anti-inflammatory drugs; OA, osteoarthritis; OARSI, Osteoarthritis Research Society International; PPAR $\gamma$ , peroxisome proliferator-activated receptor  $\gamma$ ; RA, rheumatoid arthritis; ROS, reactive oxygen species; S&F, safranin O-fast green; Tb.N, trabecular number; Tb.Sp, trabecular separation; Tb.Th, trabecular thickness; TLRs, toll-like receptors; TNF- $\alpha$ , tumor necrosis factor- $\alpha$

<sup>\*</sup>Corresponding authors. Tel.: +86 21 53315397; fax: +86 21 63137020.

E-mail addresses: [betterchiao@sjtu.edu.cn](mailto:betterchiao@sjtu.edu.cn) (Han Qiao), [ttt@sjtu.edu.cn](mailto:ttt@sjtu.edu.cn) (Tingting Tang).

<sup>†</sup>These authors made equal contributions to this work.

Peer review under responsibility of Institute of Materia Medica, Chinese Academy of Medical Sciences and Chinese Pharmaceutical Association.

<https://doi.org/10.1016/j.apsb.2019.01.015>

2211-3835 © 2019 Chinese Pharmaceutical Association and Institute of Materia Medica, Chinese Academy of Medical Sciences. Production and hosting by Elsevier B.V. This is an open access article under the CC BY-NC-ND license (<http://creativecommons.org/licenses/by-nc-nd/4.0/>).

promoted M2 macrophages in the synovium, inhibited subchondral bone destruction and reduced articular cartilage damage induced by ACLT. All the results indicated that Kin is an effective therapeutic candidate for OA treatment.

© 2019 Chinese Pharmaceutical Association and Institute of Materia Medica, Chinese Academy of Medical Sciences. Production and hosting by Elsevier B.V. This is an open access article under the CC BY-NC-ND license (<http://creativecommons.org/licenses/by-nc-nd/4.0/>).

## 1. Introduction

As the most prevalent chronic musculoskeletal disease, osteoarthritis (OA) is characterized by the progressive degeneration of articular cartilage<sup>1</sup> and afflicts patients with significantly increased joint disability<sup>2</sup>. Numerous influential factors contribute to the slow devastation of cartilage in OA including synovial inflammation, subchondral remodeling and macrophage activation<sup>3–6</sup>. Therefore, apart from the joint replacement surgery that is normally definitive treatment for OA patients in the advanced or end-stage<sup>7</sup>, conservative pharmacological treatments such as non-steroidal anti-inflammatory drugs (NSAIDs) are widely used to relieve articular inflammation<sup>8</sup>. However, the deployment of NSAIDs is largely restrained because of the inevitable side effects. Hence, further exploration of novel therapeutic targets in OA for the development of more effective treatment strategies is imperative.

Macrophages actively participate in the pathophysiological processes of various chronic bone diseases such as gouty arthritis (GA), rheumatoid arthritis (RA) and OA<sup>9–12</sup>. Macrophages play important roles in inflammation reactions that are crucial for the rehabilitation processes of musculoskeletal tissues<sup>13,14</sup>, immune defense and tissue repair<sup>9</sup>. Macrophages can be polarized to M1/M2 phenotypes according to the microenvironment. Specifically, M1 macrophages are classically activated by the stimulation of toll-like receptors (TLRs) through bacterial lipopolysaccharides (LPS) and the cytokine interferon- $\gamma$  (IFN- $\gamma$ )<sup>15</sup>. M1 macrophages have high secretion of pro-inflammatory cytokines, including IL-1 $\beta$ , IL-6, tumor necrosis factor- $\alpha$  (TNF- $\alpha$ ), IL-12, reactive oxygen species (ROS) and inducible nitric oxide synthase (iNOS)<sup>16</sup>. Nonetheless, other mediators, such as IL-4, IL-10 and IL-13, cause macrophages to polarize to the M2 type, which features high release of arginase-1 (Arg-1) and IL-10 to trigger anti-inflammatory and immunosuppressive responses<sup>17,18</sup>. Moreover, macrophage M1/M2 polarization dynamically adapts to changes in the microenvironments, showing macrophage polarization is plastic<sup>19</sup>.

Based on research to date, in physiologic synovial joints, macrophages usually remain quiescent along with fibroblasts, whereas they can be polarized into the pro-inflammatory M1 phenotype under OA inflammatory stimulus<sup>20</sup>. Therefore, targeting macrophage polarization during OA onset might emerge as an efficient therapeutic remedy *via* reversing pro-inflammatory M1 macrophages to the anti-inflammatory M2 phenotype, thereby decreasing the expression of detrimental inflammatory stimulus against chondrocytes.

However, only limited reports illustrate effective macrophage targeting strategies during OA treatment. Kinsenoside (Kin) derived from the traditional Chinese medicinal herb *Anoectochilus roxburghii* is an active small-molecule component used clinically to treat liver disease, hyperglycemia and cancers<sup>21–23</sup>. Our previous study utilizing microfluidic chips showed that Kin was the most effective anti-inflammatory component in protecting

human umbilical vein endothelial cells (HUVECs) from monosodium urate (MSU) crystal damage<sup>11</sup>. However, whether Kin can affect macrophage polarization to inhibit OA progression remains unknown. Hence, we investigated the effects of Kin treatments on M1/M2 macrophage polarization and evaluated the resulting protection of chondrocytes to attenuate OA progression. Additionally, the underlying mechanisms by which Kin repolarizes macrophages and protects chondrocytes were assessed.

## 2. Materials and methods

### 2.1. Cells, media and reagents

Primary mouse chondrocytes and RAW264.7 macrophage cell lines were cultured with Dulbecco's minimum essential medium (DMEM; HyClone, Logan, UT, USA) containing 10% fetal bovine serum (Gibco, New York, USA), penicillin at 100 U/mL (Gibco) and streptomycin at 100  $\mu$ g/mL (Gibco) at 37 °C in humidified conditions with 5% CO<sub>2</sub>. Kin was purchased from Shifeng Biological Technology Company (Shanghai, China). Bacterial LPS of *Escherichia coli* and recombinant mouse IL-1 $\beta$ , IL-4, and IFN- $\gamma$  were purchased from PeproTech (Rocky Hill, NJ, USA). IL-1 $\beta$ , IL-6, and TNF- $\alpha$  ELISA kits were purchased from R&D systems (Minneapolis, MN, USA), and iNOS and Arg-1 ELISA kits were purchased from Biovision Inc. (Palo Alto, CA, USA).

### 2.2. Chondrocytes culture and identification

Male C57BL/6J mice were sacrificed and disinfected in 75% alcohol for 10 min. The femur head was exposed under aseptic conditions, and the total articular cartilage was further isolated, collected and cut into 1 mm<sup>3</sup> pieces. The tissue was digested with 0.25% trypsin and 0.2% collagenase II for 30 min and 5 h respectively at 37 °C. Cells were then filtered through a 70  $\mu$ m cell strainer and washed 3 times with sterile phosphate-buffered saline (PBS). Afterward, the collected chondrocytes were seeded into culturing dishes in DMEM at 37 °C and 5% CO<sub>2</sub>. Culture medium was changed every 2–3 days. Primary chondrocytes were identified by immunofluorescence staining with collagen type II and aggrecan (Santa Cruz, CA, USA) before used in subsequent experiments. Only primary or passaged one generation of chondrocytes were used for experimental procedures.

### 2.3. Effects of Kin on cell viability

Effects of Kin on various cell viabilities were assessed by CCK-8. RAW264.7 macrophages (8  $\times$  10<sup>3</sup>/well) seeded in 96-well plates were treated with various concentrations of Kin for 24 h. Primary chondrocytes (6  $\times$  10<sup>3</sup>/well) seeded in 96-well plates

were treated with various concentrations of Kin for 2, 24, 48, and 72 h or with IL-1 $\beta$  (10 ng/mL) and Kin for 24 h. One hundred microliters of 10% CCK-8 (DOJINDO, Japan) solution was added to each well. Then, the absorbance was measured at 450 nm using a microplate reader (Bio-Rad, Hercules, CA, USA).

#### 2.4. Macrophage repolarization from M1 to M2 phenotype

To assess macrophage repolarization from M1 to M2, RAW264.7 macrophages were stimulated with LPS plus IFN- $\gamma$  24 h to display the M1 phenotype. Subsequently, the M1 macrophages were treated with various concentrations of Kin for additional 24 h. The polarization transitions were evaluated with quantitative real-time polymerase chain reaction (qRT-PCR), confocal observation and flow cytometry analysis.

#### 2.5. Effects of Kin on M2 macrophage polarization

RAW264.7 macrophages ( $5 \times 10^5$ /well) seeded in 6-well plates were stimulated with 20 ng/mL IL-4 for 24 h for M2 macrophage differentiation. During polarization, macrophages were further administered with different concentrations of Kin to assess Kin treatment on M2 polarization.

#### 2.6. QRT-PCR

Total RNA was extracted from primary chondrocytes and macrophages in different groups using TRIzol reagent (Invitrogen, CA, USA), and transcription-PCR was performed by real-time PCR (ABI 7500, CA, USA). The primers used are listed in [Supporting information Table 1](#). Values were normalized to *Gapdh* mRNA levels and calculated by  $2^{-\Delta\Delta Ct}$ .

#### 2.7. Immunofluorescent staining

Treated with Kin for 24 h, polarized RAW264.7 cells were fixed in paraformaldehyde with 0.1% Triton X-100 (Sigma, USA). Goat serum (4%) was used to block nonspecific binding. Then, cells were incubated with CD16/32 and CD206 primary antibodies (BD, CA, USA; dilution 1:200) overnight. The fluorescent secondary antibodies were used to visualize the corresponding subsets. Further, cells were stained in 4,6-diamidino-2-phenylindole (DAPI) for 5 min; cells were observed under a confocal fluorescence microscope (Leica TCS-SP5, DM6000-CFS). We identified CD16/32 positive cells as M1 macrophages and CD206 positive cells as M2 macrophages.

#### 2.8. Flow cytometry for macrophage subset analysis

To distinguish macrophage M1 and M2 polarization transitions after Kin treatments, CD16/32 was chosen to mark the M1 phenotype and CD206 for the M2 phenotype. Alexa Fluor 647-conjugated anti-CD206 (BD, CA, USA) and PE-conjugated anti-CD16/32 (BD) were used to evaluate macrophage subsets. Alexa Fluor 647 rat isotype control and PE rat isotype control (BD) were used to distinguish the positive cells. Samples were further analyzed using a FACScan flow cytometer (BD).

#### 2.9. Western blot

Pre-polarized macrophages were treated with various concentrations of Kin. The proteins were extracted and used for Western blot analyses as reported previously<sup>24</sup>.

#### 2.10. Macrophage conditioned medium (CM) collection and stimulation

RAW264.7 macrophages were stimulated with LPS plus IFN- $\gamma$  to display the M1 phenotype and IL-4 for M2 macrophage differentiation for 24 h. Polarized macrophages supernatants were harvested and subjected to centrifugation at a speed of  $1000 \times g$  for 5 min and stored at  $-80^\circ\text{C}$  for further experiments. The CM from differentiated macrophages was diluted at the ratio of 1:1 with serum-free medium and added to chondrocytes for further analyses.

#### 2.11. Cytokine measurements

Pre-polarized RAW264.7 macrophages were treated with Kin (6.25–25  $\mu\text{g/mL}$ ) for 24 h. The CM of macrophages was collected, and the concentrations of IL-1 $\beta$ , IL-6 and TNF- $\alpha$  and iNOS and Arg-1 were measured via ELISA kits according to the manufacturer's guidelines.

#### 2.12. Safranin O-fast green (S&F) and toluidine blue staining of chondrocytes

Primary mice chondrocytes ( $1 \times 10^6$ /well) seeded in 6-well plates were cultured in the CM of macrophages for 3 days. Chondrocytes were treated with or without IL-1 $\beta$  (10 ng/mL) and various concentrations of Kin for 24 h. S&F and toluidine blue staining were performed according to the manufacturer's instructions.

#### 2.13. Flow cytometry for chondrocyte apoptosis analysis

Chondrocytes ( $10^6$ /well) seeded in 6-well plates were stimulated with or without IL-1 $\beta$  (10 ng/mL) and various concentrations of Kin for 24 h. Chondrocytes in another 6-well plate were treated with CM of macrophages for 3 days. Chondrocyte apoptosis rates were analyzed with annexin V-FITC/propidium iodide (PI) double staining (BD) according to the manufacturer's instructions.

#### 2.14. Mice knee OA model induced by anterior cruciate ligament transection (ACLT)

Thirty 2-month-old male C57BL/6J mice were purchased from Shanghai SLAC Laboratory Animal Company (Shanghai, China) and fed on commercial food and provided water in specific pathogen-free conditions approved by the Animal Ethical Committee of Shanghai Ninth People's Hospital. All animal experiments complied with National Institutes of Health guide for the care and use of Laboratory animals. The ACLT-induced abnormal mechanical loading-associated OA of the right knee was established according to previous research<sup>25,26</sup>. The sham operation was performed by only opening the joint capsule and then suturing the incision. The thirty mice were randomly split into five groups, with six mice per cage. The mice in group 1 mice were treated with the sham operation as the control group. For groups 2–5, ACLT was administered to the right knee of mice. Mice in group 2 were

injected intraperitoneally with PBS, and those in groups 3–5 were injected intraperitoneally with Kin at the concentrations of 2.5, 5, and 10 mg/kg body weight every other day for 4 weeks. The concentrations of Kin used *in vivo* were based on our previous studies<sup>11</sup>.

### 2.15. Evaluations with micro-CT scanning

At 4 weeks post-injections, knee joints of mice were harvested and fixed in 4% paraformaldehyde. Specimens were scanned using micro-CT ( $\mu$ CT 40; Scanco, Zurich, Switzerland) as described previously<sup>27</sup>. We set the scanner at a resolution of 10  $\mu$ m with voltage, 70 kV; electric current, 114  $\mu$ A. We defined the region of interest (ROI) to cover the whole subchondral bone in tibial plateaus. Three-dimensional structural parameters analyzed included bone volume (BV), bone volume/total tissue volume (BV/TV), and trabecular number (Tb.N), thickness (Tb.Th) and separation (Tb.Sp).

### 2.16. Histological observation

Samples were decalcified in 10% EDTA and then embedded in paraffin. Sagittal sections were cut to a 4  $\mu$ m thickness of the knee joint medial compartment and processed with hematoxylin & eosin (H&E) and S&F. Osteoarthritis Research Society International (OARSI) and synovitis scores were calculated as previously<sup>28,29</sup>. Immunohistochemical staining was accomplished with antibodies against F4/80, CD16/32 and CD206 (BD; dilution 1:200), aggrecan (Abcam, Cambridge, MA, USA; dilution 1:100), cleaved caspase-3 (Abcam; dilution 1:500), MMP-3 (Santa Cruz; dilution 1:100), IL-1 $\beta$  (Abcam; dilution 1:200), and TNF- $\alpha$  (Abcam; dilution 1:200). Samples were stained with diaminobenzene (Dako, North Sydney, NSW, Australia) and counterstained with hematoxylin (Sigma, St. Louis, MO, USA). Images were captured using a Zeiss Axio Imager light microscope. The number of positively stained cells was counted in per specimen and three sequential specimens in each group were measured. Three sequential specimens per mouse in each group were measured.

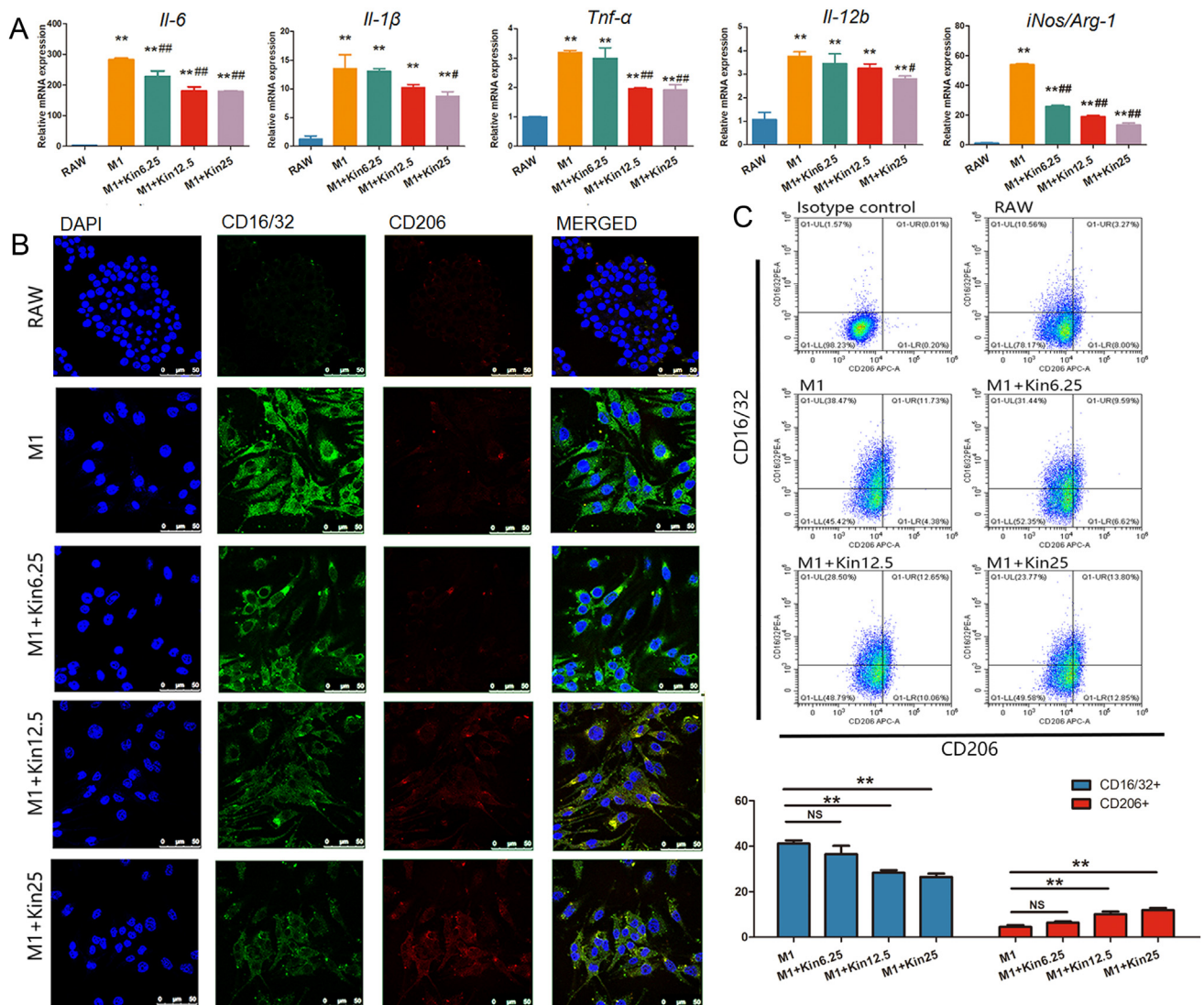


**Figure 1** Effects of Kin on macrophage repolarization *in vitro*. (A) QRT-PCR was conducted to determine the expression levels of the M1-related genes IL-6, IL-1 $\beta$ , TNF- $\alpha$ , IL-12 and iNOS/Arg-1. (B) M1 macrophage marker CD16/32 and M2 macrophage marker CD206 were examined by immunostaining. (C) Flow cytometry evaluated macrophage subsets by staining CD16/32 and CD206. \* $P < 0.01$  compared with RAW264.7 group; # $P < 0.05$ , ## $P < 0.01$  compared with M1 group. Scale = 50  $\mu$ m.

### 2.17. Statistical analyses

All data are expressed as the mean  $\pm$  standard deviation. One-way analysis of variance (ANOVA) was used for multifactorial comparisons in this study. A  $P$  value  $<0.05$  were considered statistically significant. \* and # denote  $P < 0.05$ , and \*\* and ## denote  $P < 0.01$ . All data analysis was conducted with the SPSS 22.0 statistical software package (SPSS Inc, Chicago, IL, USA).

## 3. Results

### 3.1. Kin repolarizes M1 type macrophages to M2 phenotype

The formula for the chemical structure of Kin is presented in Supporting Information Fig. S1A. As shown in Supporting Information Fig. S1B, macrophage viability after Kin treatments showed that 3.125, 6.25, 12.5, 25, and 50  $\mu\text{g/mL}$  Kin had minimal effects on RAW264.7 macrophages. Based on qRT-PCR results, Kin decreased the expression of M1-related genes IL-6, IL-1 $\beta$ , TNF- $\alpha$ , IL-12 and iNOS/Arg-1 in a dose-dependent manner (Fig. 1A).

Immunofluorescent observations showed that Kin suppressed CD16/32 positive cells (M1 macrophages), whereas CD206 positive cells (M2 macrophages) were promoted (Fig. 1B). Based on flow cytometry, the percent of CD16/32 positive cells (M1 macrophages) in the LPS+IFN- $\gamma$  group was  $41.16 \pm 2.45\%$ , which was reduced to  $36.48 \pm 6.49\%$ ,  $28.33 \pm 1.95\%$ , and  $26.49 \pm 2.59\%$  in the Kin 6.25, 12.5 and 25  $\mu\text{g/mL}$  treated groups, respectively. The percentage of CD206 positive cells (M2 macrophages) increased  $10.01 \pm 2.06\%$  and  $11.84 \pm 1.80\%$  in the 12.5 and 25  $\mu\text{g/mL}$  concentrations of Kin-treated groups respectively, which was significantly ( $P < 0.05$ ) more than that in the M1 group (Fig. 1C). These data showed Kin moderately repolarized M1 macrophages to the M2 phenotype.

### 3.2. Macrophage repolarization by targeting NF- $\kappa$ B and MAPK signals via Kin

Western blot analysis of macrophages revealed that LPS+IFN- $\gamma$  markedly activated the phosphorylation of IKK, I $\kappa$ B $\alpha$  and p65 in NF- $\kappa$ B signaling. Kin did not affect the expression of phosphorylated IKK in varying groups, whereas the downstream

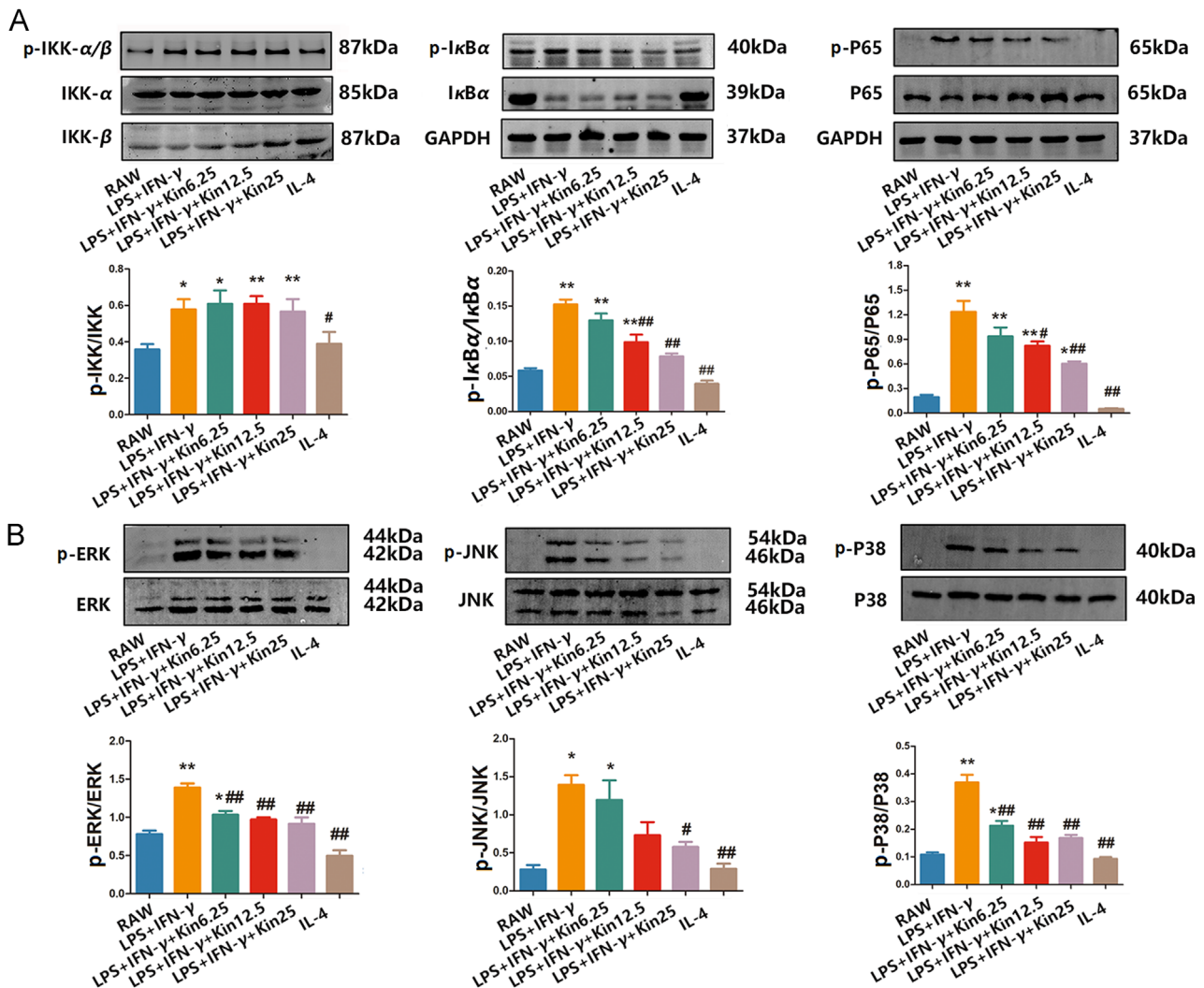


**Figure 2** Effects of Kin on signaling pathways related to macrophage polarization. Western blot showed that Kin affected NF- $\kappa$ B signal-related proteins IKK/p-IKK, I $\kappa$ B $\alpha$ /p-I $\kappa$ B $\alpha$ , and P65/p-P65 (A) and MAPK signal-related proteins p-JNK/JNK, p-ERK/ERK and p-P38/P38 (B). \* $P < 0.05$ , \*\* $P < 0.01$  compared with RAW264.7 group; # $P < 0.01$ , ## $P < 0.01$  compared with the 100 ng/mL LPS plus 20 ng/mL IFN- $\gamma$  group.

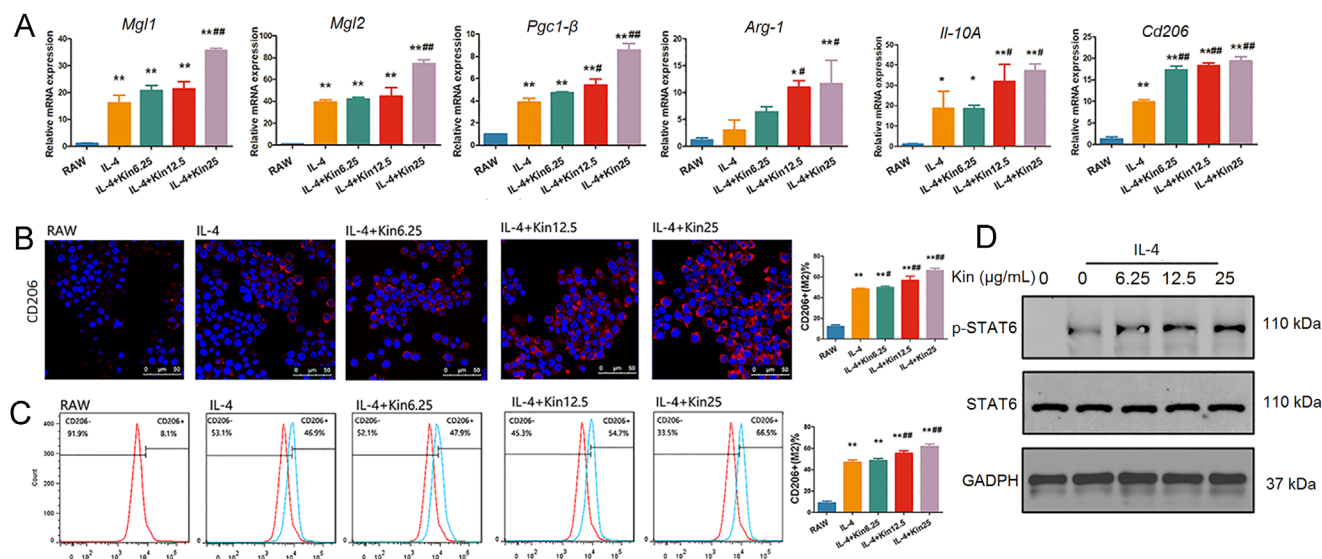


**Figure 3** Effect of Kin on M2 macrophage polarization. M2-related genes *Mgl1*, *Mgl2*, *Pgc1-β*, *Arg-1*, *Il-10* and *Cd206* were assessed by qRT-PCR (A). (B) M2 macrophage marker CD206 was examined by immunostaining. (C) Flow cytometry evaluated macrophage subsets by staining CD206. (D) The expression of p-STAT6/STAT6 was assessed by Western blot. Scale=50 μm.

phosphorylation of both IκBα and P65 was inhibited by Kin administration dose-dependently (Fig. 2A), indicating that Kin may target IKK-α and IKK-β kinases, further affecting the function of p-IKK. These results are consistent with our previous study in which Kin could bind to specific sites of IKK-α and IKK-β in a molecular docking assay<sup>11</sup>. In the MAPK pathway, phosphorylation of ERK, JNK, and P38 was up-regulated when LPS+IFN-γ was administered; whereas Kin reduced the expression of p-JNK, p-Erk, and p-p38 dose-dependently (Fig. 2B). Moreover, IL-4, as the mediator of M2 macrophage activation, failed to activate the phosphorylation of kinases in NF-κB/MAPK signaling in comparison with the control group, which indicated that M2 macrophage polarization was not activated by NF-κB/MAPK signal.

### 3.3. Kin promotes M2 macrophages polarization

Kin increased the expression of M2-related genes *Mgl1*, *Mgl2*, *Pgc1-β*, *Arg-1*, *Il-10* and *Cd206* (Fig. 3A). Immunofluorescence demonstrated the population of CD206 positive macrophages increased after Kin was administered (Fig. 3B). Furthermore, the percentage of M2 in the IL-4 group was  $46.9 \pm 3.76\%$ , which increased to  $48.43 \pm 3.63\%$ ,  $55.53 \pm 3.9\%$ , and  $61.7 \pm 4.25\%$  in the corresponding Kin-treated groups, showing that Kin promoted M2 macrophage polarization (Fig. 3C). Furthermore, STAT6 is an important transcription factor for M2 polarization<sup>30</sup>, we found that Kin promoted the expression of p-STAT6 in a dose-dependent manner, which could explain how Kin could promote M2 polarization (Fig. 3D).

### 3.4. Kin prevents impairment of chondrocytes from macrophage CM

ELISA results showed that LPS plus IFN-γ stimulated the expression of IL-6, IL-1β, TNF-α and iNOS in macrophages, signifying that M1-type macrophages could release several destructive factors for subsequent cartilage damage in OA. However, when macrophages were treated with varying

concentrations of Kin, the expression of these pro-inflammatory factors decreased significantly, suggesting that the Kin administered targeted M1-type macrophages to reduce relevant releases of destructive factors, thereby providing promising possibilities for subsequent cartilage protection (Fig. 4A). Hence, we further utilized the CM of macrophages to treat primary chondrocytes. Primary chondrocytes were identified by immunofluorescence for aggrecan (Supporting Information Fig. S2A) and collagen type II (Supporting Information Fig. S2B) of mice. Based on the results obtained after 3 days of co-culture, the number of chondrocytes increased with the treatment of Kin compared with that of the LPS+IFN-γ-CM group, as shown by the increase in staining intensity of S&F and toluidine blue staining (Fig. 4B and C). Flow cytometry indicated that the apoptosis rate was  $19.65 \pm 0.78\%$  in the LPS+IFN-γ-CM group, which was greater than the  $3.41 \pm 0.78\%$  in the RAW-CM group. In the 6.25, 12.5, and 25 μg/mL Kin-treated groups, the apoptosis rate was significantly ( $P < 0.05$ ) reduced to  $11.66 \pm 1.60\%$ ,  $9.63 \pm 2.22\%$ , and  $8.89 \pm 1.92\%$ , respectively, which demonstrated that Kin could exert a dose-dependent beneficial effect on macrophage CM-induced chondrocyte apoptosis (Fig. 4D). Moreover, the observations of chondrocyte viabilities after combined treatments of LPS+IFN-γ-CM with Kin confirmed the result, showing that the cell viabilities of chondrocytes were rescued with Kin administered after LPS+IFN-γ-CM stimulation (Fig. 4E). These results were also confirmed with Western blotting, which indicated that both the BAX (pro-apoptotic proteins)/BCL-2 (anti-apoptotic proteins) ratio and the pro-apoptotic proteins cleaved caspase-3/caspase-3 ratio decreased under the treatments with Kin compared with those in the LPS+IFN-γ-CM group (Fig. 4F).

### 3.5. Kin inhibits IL-1β-induced chondrocyte apoptosis

The viabilities of chondrocytes were measured after Kin treatments for 2, 24, 48, and 72 h. The results showed that low concentrations of Kin (3.125, 6.25, 12.5, and 25 μg/mL) had minimal inhibitory effects on chondrocytes, whereas concentrations of 100 and 200 μg/mL Kin significantly inhibited cell proliferation at 24, 48, and

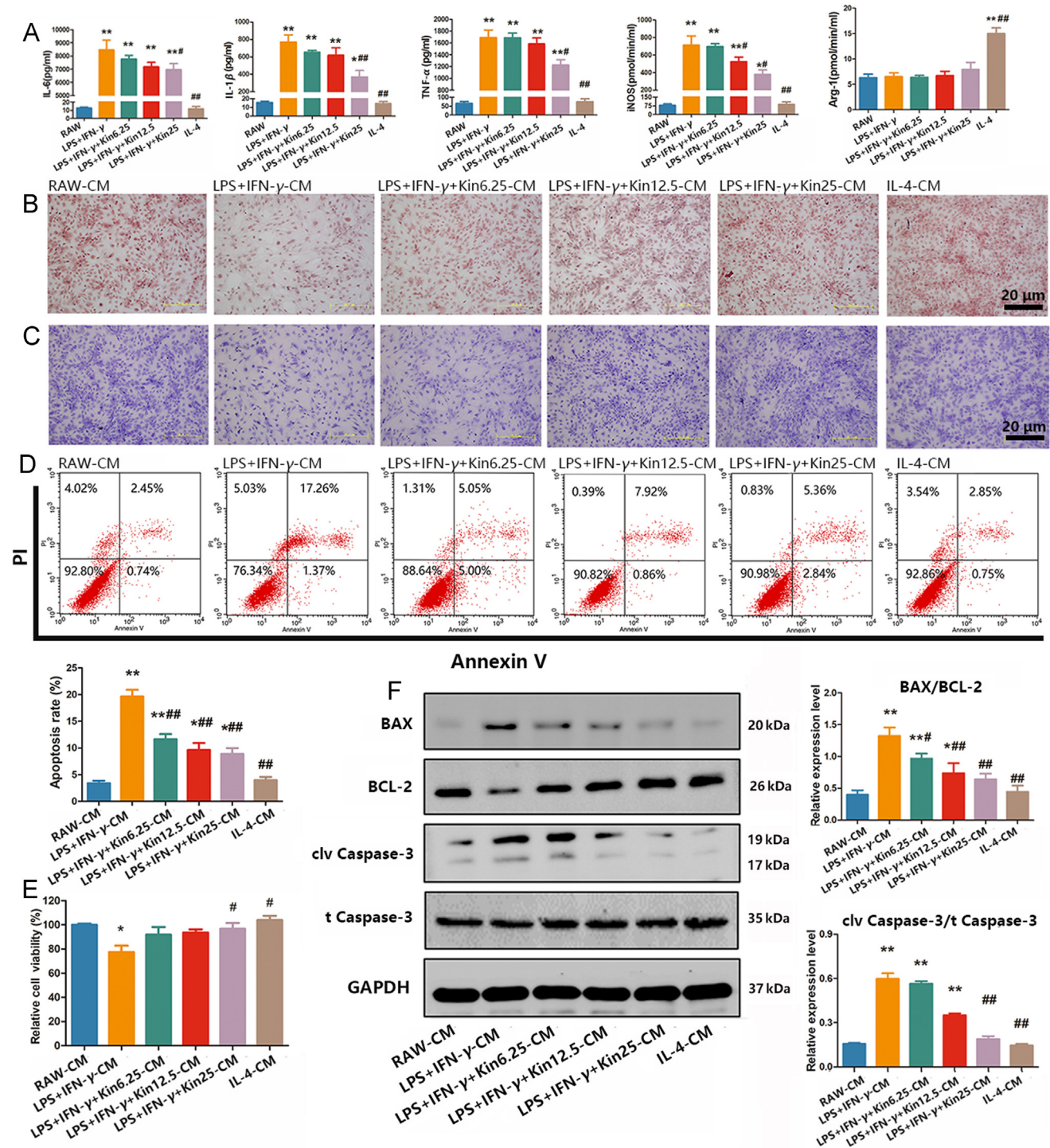


**Figure 4** Macrophage CM and co-culture with chondrocytes. For the co-culture assay, the components of macrophage CM (IL-6, IL-1 $\beta$ , TNF- $\alpha$ , iNOS and Arg-1) were measured by ELISA kit (A). S&F (B) and toluidine blue staining (C) in chondrocytes cultured with macrophage CM for 3 days. (D) Apoptosis rates for macrophage CM-stimulated chondrocytes were analyzed by flow cytometry with annexin V-FITC/PI apoptosis analysis. (E) Cell viability was evaluated in chondrocytes treated with macrophage CM by CCK-8. (F) Apoptosis-related proteins (BAX, BCL-2, cleaved caspase-3, caspase-3) were monitored by western blot. \* $P < 0.05$ , \*\* $P < 0.01$  compared with RAW264.7-CM group; # $P < 0.05$ , ## $P < 0.01$  compared with LPS+IFN- $\gamma$ -CM group. Scale = 20  $\mu$ m.

72 h. However, 50  $\mu$ g/mL Kin only inhibited cell proliferation at 72 h (Supporting Information Fig. S3A). Furthermore, Kin treatments of 6.25, 12.5, and 25  $\mu$ g/mL obviously protected chondrocytes from IL-1 $\beta$ -induced proliferation inhibition (Fig. S3B). S&F

(Fig. S3C) and toluidine blue staining (Fig. S3D) showed Kin treatment increased staining intensity compared with that of the IL-1 $\beta$  group, indicating the number of chondrocytes increased with Kin treatment under IL-1 $\beta$  stimulation.

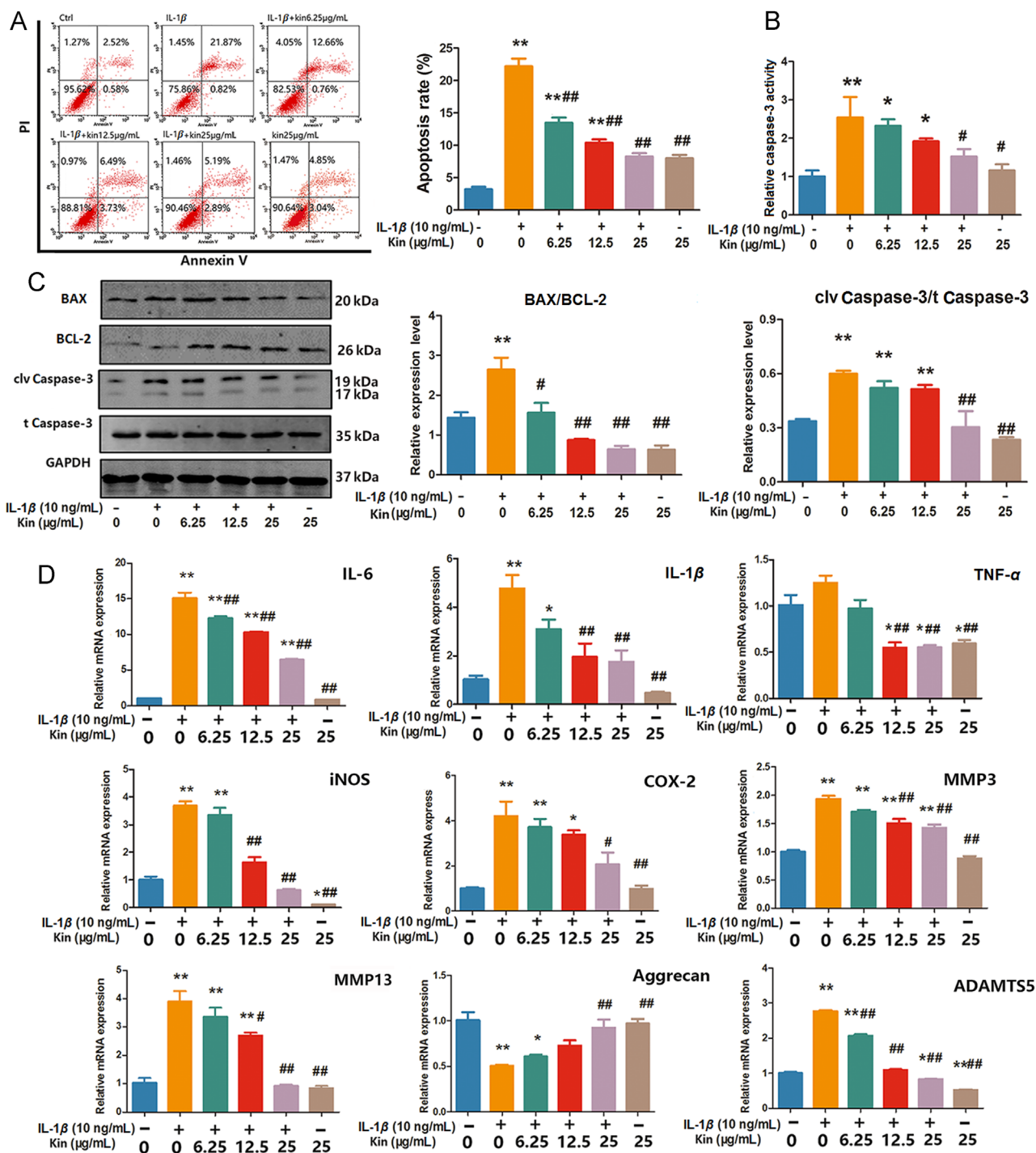


**Figure 5** Effects of Kin on IL-1 $\beta$ -induced chondrocyte apoptosis and expression of related genes. (A) Apoptosis rates for IL-1 $\beta$ -stimulated chondrocytes were analyzed by flow cytometry with annexin V-FITC/PI analysis. (B) The caspase-3 activity was detected by the caspase-3 activity assay. Absorbance at 405 nm was used to quantify caspase-3 activation. The results were normalized to the control group. (C) Apoptosis-related proteins (BAX, BCL-2, cleaved caspase-3, caspase-3) were evaluated with Western blot. (D) QRT-PCR was performed to determine the expression levels of IL-6, IL-1 $\beta$ , TNF- $\alpha$ , iNOS, COX-2, MMP-3, MMP-13, aggrecan and ADAMTS5 in chondrocytes under IL-1 $\beta$  stimulation. \* $P$  < 0.05, \*\* $P$  < 0.01 compared with 0  $\mu$ g/mL Kin; # $P$  < 0.05, ### $P$  < 0.01 compared with the 10 ng/mL IL-1 $\beta$  group.

Flow cytometry (Fig. 5A) and caspase-3 activity assay (Fig. 5B) demonstrated that Kin treatments (6.25–25  $\mu$ g/mL) exerted beneficial effects on IL-1 $\beta$ -induced chondrocyte apoptosis. In the IL-1 $\beta$  group, the apoptosis rate was  $22.23 \pm 2.03\%$ , which was reduced to  $13.47 \pm 1.40\%$ ,  $10.38 \pm 0.90\%$ , and  $7.25 \pm 0.94\%$  in the Kin 6.25, 12.5,

and 25  $\mu$ g/mL treated groups, respectively. These results were also confirmed with Western blotting (Fig. 5C), which showed both the BAX/BCL-2 ratio and the pro-apoptotic proteins cleaved caspase-3/caspase-3 ratio increased in the IL-1 $\beta$  group, whereas the ratios decreased in Kin treatment groups dose-dependently.

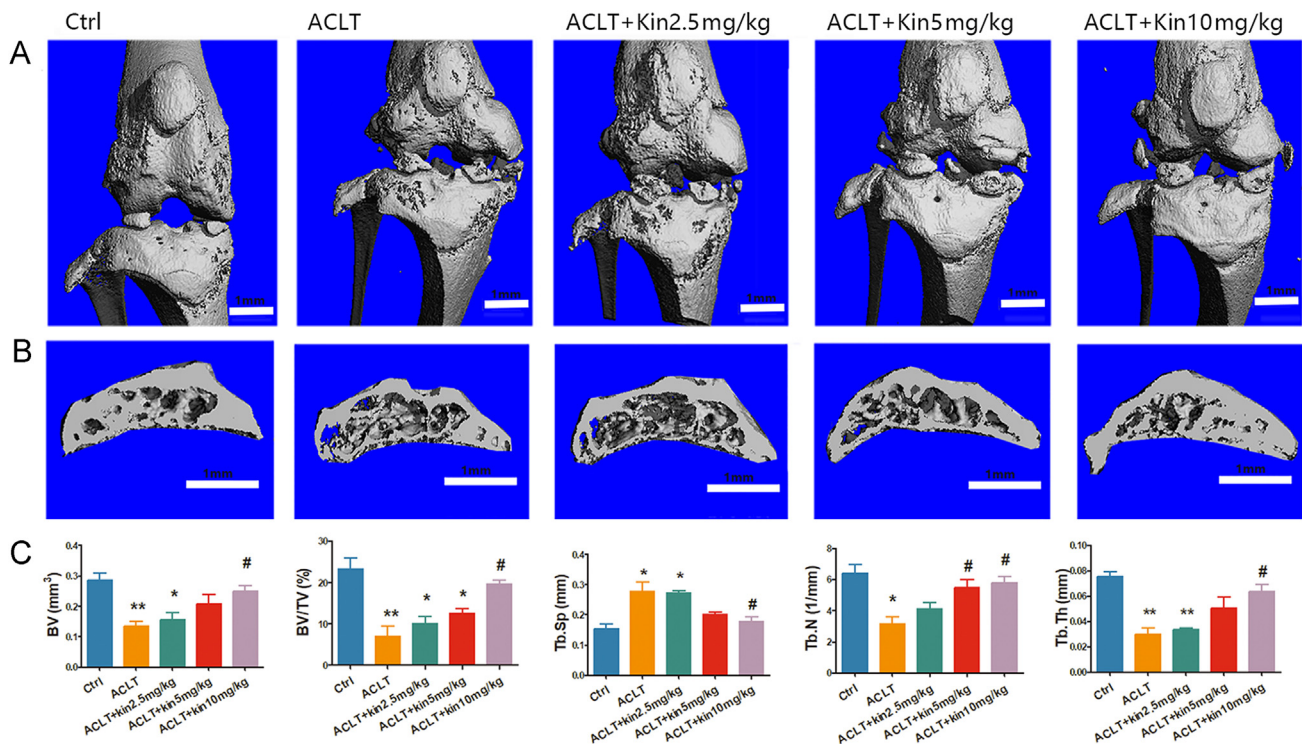


**Figure 6**  $\mu$ CT evaluations of Kin-treated OA induced by ACLT. (A) Three-dimensional  $\mu$ CT images of frontal views of the knee joints at 4 weeks after sham operation or ACLT operation. (B) Sagittal views of medial compartment subchondral bone. (C) Quantitative analysis of BV, BV/TV, Tb.Sp, Tb.N and Tb.Th. \* $P < 0.05$ , \*\* $P < 0.01$  compared with the control group, # $P < 0.05$  compared with the ACLT group. Scale = 1 mm.

### 3.6. Kin reduces IL-1 $\beta$ -induced inflammatory and degenerative cytokines expression in chondrocytes

For mRNA levels, qRT-PCR results showed that IL-1 $\beta$  drastically stimulated the levels of the inflammatory cytokines IL-6, IL-1 $\beta$ , TNF- $\alpha$ , iNOS and COX-2, in addition to varying cartilage destructive factors MMP-3, MMP-13 and ADAMTS5 in chondrocytes. However, IL-1 $\beta$  significantly down-regulated the production of aggrecan, showing that IL-1 $\beta$  could be the primary pathological caused in cartilage destruction during OA development. Nonetheless, we found that Kin treatments (6.25–25  $\mu$ g/mL) reduced the expression of IL-6, IL-1 $\beta$ , TNF- $\alpha$ , iNOS, COX-2, MMP-3, MMP-13 and ADAMTS5, whereas the expression of the protective aggrecan increased in a dose-dependent manner (Fig. 5D), demonstrating that Kin could be a potential drug to reduce inflammation and delay degeneration.

### 3.7. Kin decreases bone resorption induced by anterior cruciate ligament transection *in vivo*

In early stage of OA, bone loss is associated with increased bone remodeling<sup>51</sup>. To investigate the effects of Kin on the subchondral bone remodelling of OA, we administered Kin intraperitoneally in mice after ACLT. Result signified that ACLT injury induced significant bone resorption, as shown by the increased osteolysis in subchondral bone of tibia. Nonetheless, Kin treatments reduced bone loss dose-dependently, showing increased integrity of the knee bone and bone mass in subchondral bone, indicating that osteolysis was diminished after Kin administered *in vivo* (Fig. 6A and B). Statistically, the BV of subchondral bone in tibial plateau was  $0.14 \pm 0.03$  mm<sup>3</sup> in the ACLT group, which was significantly

( $P < 0.05$ ) lower than the  $0.29 \pm 0.04$  mm<sup>3</sup> of the control group. Nonetheless, in 2.5, 5 and 10 mg/kg Kin-treated mice, BV was  $0.15 \pm 0.04$ ,  $0.21 \pm 0.05$ , and  $0.25 \pm 0.03$  mm<sup>3</sup>, respectively. BV and the other parameters including BV/TV, Tb.N, Tb.Th and Tb.Sp showed the suppressed bone destruction effect of Kin *in vivo* (Fig. 6C).

### 3.8. Kin attenuates the progression of OA in ACLT mice

ACLT induced an increase in the thickness of synovial lining cells, whereas Kin reduced dose-dependently the thickness of lining cells and synovial inflammation (Fig. 7A and A1). Macrophages stained by F4/80 in synovium were increased in the ACLT group, while Kin dose-dependently decreased the infiltration of macrophages (Fig. 7B). Specifically, we found that the infiltration of pro-inflammatory M1 macrophages (CD16/32 positive cells) in the synovium was increased in the ACLT group, whereas Kin obviously reduced the number of M1 macrophages in Kin-treated OA mice (Fig. 7C). Additionally, Kin up-regulated the number of M2-type macrophages (CD206 positive cells) in the synovium (Fig. 7D) and decreased the expression of IL-1 $\beta$  and TNF- $\alpha$  in the synovium (Supporting Information Fig. S4A and B).

S&F and H&E staining demonstrated the loss of proteoglycan and decreased thickness of articular cartilage induced by ACLT surgery. However, in Kin-treated ACLT mice, the degeneration of cartilage was inhibited significantly (Fig. 7E and F). Moreover, Kin attenuated the loss of aggrecan (Fig. 7G) induced by ACLT, and the expression of cleaved caspase-3, MMP-3, IL-1 $\beta$  and TNF- $\alpha$  were also decreased in articular cartilage after Kin treatment (Fig. S4C–F).

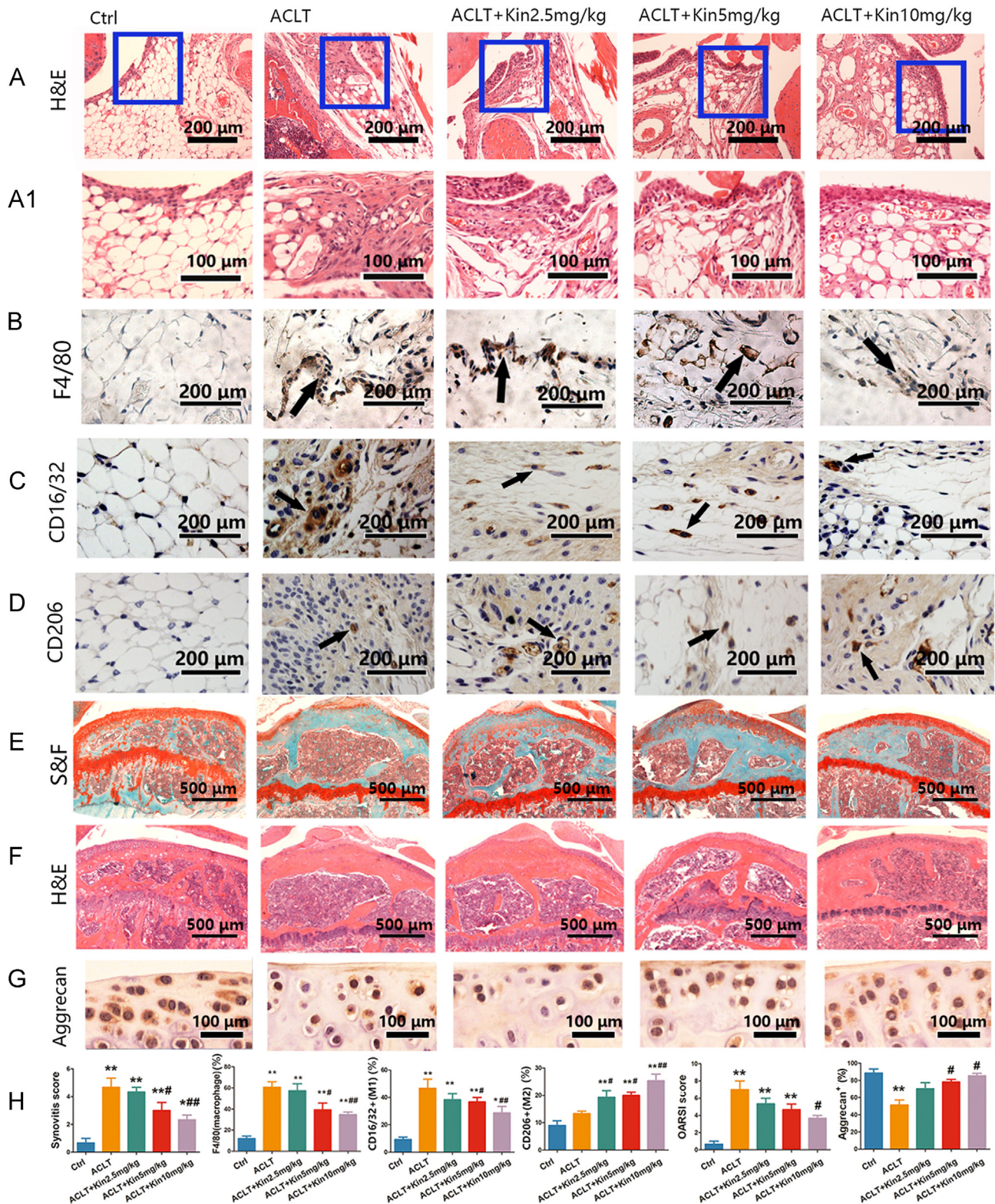


**Figure 7** Staining evaluations of Kin in OA induced by ACLT. (A) and (A1) Synovial membrane of medial compartment was stained with H&E. Synovial macrophages were identified by F4/80 (B) immunohistochemistry, moreover, CD16/32 (C) was chosen for marking M1-type macrophages and CD206 (D) for M2-type macrophages. Medial compartment cartilage and subchondral bone of knee joints were stained by S&F (E) and H&E (F). Aggrecan immunohistochemistry of knee joint medial compartment cartilage (G). (H) Quantitative analysis of synovitis score, synovial macrophages M1 and M2, OARSI score and aggrecan. \* $P < 0.05$ , \*\* $P < 0.01$  compared with the control group; # $P < 0.05$ , ### $P < 0.01$  compared with the ACLT group.

#### 4. Discussion

OA is typically characterized by degeneration and loss of articular cartilage, but involves all tissues of the joint including subchondral bone and synovial membrane<sup>32</sup>. In early stage of OA, bone loss is associated with increased bone remodeling<sup>31</sup>. Increasing evidence showed that osteoclast activity is increased in early OA, disturbing the equilibrium between bone formation and resorption, which could finally lead to a marked reduction in subchondral bone thickness<sup>33,34</sup>. Furthermore, the reduction in the thickness of the subchondral plate was associated with increased articular cartilage destruction<sup>35</sup>. This progression was followed by slow densification of the subchondral plate and loss of cartilage. In late stage, OA is characterized by decreased bone resorption and development of subchondral sclerosis. With the subchondral plate thickening, increasing loss of aggrecan leads to the reduction of the thickness of non-mineralized articular cartilage<sup>31</sup>.

Currently, various therapeutic approaches are applied to treat OA<sup>36</sup>. Despite many studies that attempt to attenuate articular inflammation and delay cartilage degeneration<sup>37</sup>, no effective treatment has yet focused on the vital roles of macrophages during OA development<sup>38</sup>. In this study, we were committed to identify one promising candidate targeting macrophage repolarization for effective OA treatment.

Increasing evidence shows that synovial macrophages are the key effector cells during OA progression<sup>39</sup>. Synovial macrophages promote the production of varying pro-inflammatory cytokines such as IL-1 $\beta$ , IL-6 and TNF- $\alpha$ , which further deteriorates synovial inflammation and increases formation of osteophyte<sup>40</sup>. Additionally, macrophages can activate synovial fibroblasts to release destructive enzyme MMPs concomitantly<sup>40</sup>. Therefore, macrophages are realistic to emerge as the novel target for the treatment of OA.

Macrophages express diverse cell surface receptors, which are responsible for the recognition of intercellular signals. These receptors can be triggered by a specific stimulus, which further polarizes macrophages into pro-inflammatory-type M1 or anti-inflammatory-type M2. M1 macrophages highly express MHC II molecules and costimulatory CD80/86 molecules such as CD16/32, CD86 and CD40, which primarily are used to present antigens<sup>41</sup>. M2 macrophages show high expression of phagocytosis markers CD206 and CD163<sup>42</sup>. NF- $\kappa$ B, activator protein-1 (AP-1), and STAT1, among others, are the mediators of M1 macrophage polarization, whereas transcription factors including interferon regulatory factor 4 (IRF4), CCAAT/enhancer-binding protein  $\beta$  (C/EBP  $\beta$ ), STAT6 and peroxisome proliferator-activated receptor  $\gamma$  (PPAR $\gamma$ ) can promote M2 activation<sup>43</sup>. NF- $\kappa$ B is an important transcription factor regulating macrophage polarization on exposure to inflammation, infection and stress<sup>44</sup> and also regulates the expression of inflammatory mediators and determines cell differentiation<sup>45</sup>. Our results showed that NF- $\kappa$ B signaling was significantly activated after stimulation with LPS and IFN- $\gamma$ ; whereas Kin dose-dependently inhibited the phosphorylation of I $\kappa$ B $\alpha$  and subsequently P65. The MAPK are a serine-threonine protein kinases family containing p-JNK/JNK, p-ERK/ERK and p-P38/P38, which regulates numerous cellular activities including cell proliferation, differentiation, apoptosis, inflammation, and innate immunity<sup>46</sup>. MAPK signaling is also implicated in modulating the polarization of M1 macrophages<sup>40,43</sup>, which are important regulators in the production of inflammatory cytokines<sup>47</sup>. Such a signaling pathway can be activated by different cellular stresses such as oxidative and osmotic stress and pro-inflammatory cytokines such as IL-1 $\beta$ . Our results showed that LPS and IFN- $\gamma$  activated MAPK

signaling p-JNK, p-ERK and p-P38, whereas Kin dose-dependently inhibited the activation of MAPK signaling. M2 macrophages are activated by IL-4, IL-10 or IL-13 through the activation of STAT6<sup>48</sup>, which highly express M2 phenotype markers such as CD206 and Arg-1. In the present study, we focused on the effects of Kin on macrophage repolarization and subsequent inflammatory response and found that Kin treatment could repolarize M1 macrophages to the M2 phenotype. Furthermore, we were delighted to discover that Kin could up-regulate the M2 macrophage markers, which might increase M2 macrophage function.

Kin has been found to be a potential immunosuppressive drug which could disrupt dendritic cells (DC)-induced cross-priming of CD8<sup>+</sup> T cell responses in treatment of autoimmune hepatitis (AIH)<sup>49</sup>. Besides, Hsiao et al.<sup>50</sup> demonstrated that Kin increased the population of CD4<sup>+</sup>CD25<sup>+</sup> regulatory T cells, thereby inhibiting the Th1 cell and B cell populations in a collagen-induced arthritis (CIA) model. These signified that Kin is an immunomodulatory drug that could regulate T cells. Furthermore, Kin significantly suppressed TNF- $\alpha$ , IFN- $\gamma$ , and IL-17 while increase the concentration of IL-10 in the supernatants of splenocytes in CIA mice<sup>50</sup>. As IFN- $\gamma$  and IL-10 could stimulate macrophage polarization, it can be speculated that Kin may indirectly affect macrophages polarization by affecting regulatory T cells. However, different from RA, OA is mainly caused by mechanical instability, and macrophages in synovial membrane play an important role in the progression of OA. Herein, in this article, we were committed to research whether Kin could directly reprogram pro-inflammatory M1 macrophages to anti-inflammatory M2 phenotype. Whether Kin could regulate macrophage polarization by affecting regulatory T cells in OA is known, this may need to be further studied.

IL-1 $\beta$  is one of the most important pro-inflammatory cytokines in the development of OA, which acts as an injury factor inducing the release of inflammatory mediators and MMPs<sup>51</sup>. In OA joints, excessive production of IL-1 $\beta$  is found in synovial fluid, the synovial membrane, subchondral bone and cartilage<sup>52,53</sup>. Herein, IL-1 $\beta$  was used as active stimulus to mimic the OA inflammatory microenvironment *in vitro*. Previous study found that IL-1 $\beta$  activates NF- $\kappa$ B signaling *via* triggering I $\kappa$ B $\alpha$  phosphorylation<sup>54</sup>. Once activated, P65 dissociates from the inhibitory I $\kappa$ B $\alpha$  complex to enter the cell nucleus, which leads to the transcription of specific targeted genes such as IL-1 $\beta$ , IL-6, and COX-2<sup>55,56</sup>. Herein, we found that 10 ng/mL IL-1 $\beta$  inhibited chondrocyte proliferation and promoted apoptosis, with increased release of pro-apoptotic proteins such as caspase-3 plus BAX and reduced levels of anti-apoptotic protein BCL-2. Moreover, our results showed IL-1 $\beta$  drastically stimulated the levels of inflammatory cytokines IL-6, IL-1 $\beta$ , TNF- $\alpha$ , iNOS, and COX-2 and the expression of cartilage destructive factors MMP-3, MMP-13 and ADAMTS5 in chondrocytes, whereas Kin reduced such inflammation and delayed the following cartilage degeneration. Notably, the production of IL-1 $\beta$  increased under autocrine stimulation, indicating that IL-1 $\beta$  could act as an irritant and product simultaneously during OA progression. Additionally, we found that Kin exerted an anti-apoptotic effect on IL-1 $\beta$ -stimulated chondrocytes, which was most noticeable at the concentration of 25  $\mu$ g/mL *in vitro*. Additionally, Kin was administered systemically to target synovial macrophages, which might avoid local infection or septic arthritis caused by repeated intra-articular injection.

Our results showed that Kin played a multifunctional role in the treatment of OA. First, Kin dose-dependently attenuated pro-inflammatory macrophage release of IL-1 $\beta$ , IL-6, TNF- $\alpha$ , iNOS and IL-12, which were regulated by NF- $\kappa$ B/MAPK signaling<sup>55,56</sup>.

Even when a certain amount of a cytokine such as IL-1 $\beta$  entered into the joint cavity, Kin directly protected the cartilage from injury. Moreover, Kin reduced the production of COX-2, playing a similar role to that of NSAIDs. Therefore, Kin is a potential substitute for NSAIDs. Further, the damage effect of CM supernatants from pro-inflammatory macrophages was weakened by Kin dose-dependently.

## 5. Conclusions

In conclusion, this study demonstrated the positive role of Kin in OA treatment. Kin repolarized M1 macrophages to M2. The potential mechanism was that Kin targeted the NF- $\kappa$ B/MAPK pathway to inhibit the phosphorylation of I $\kappa$ B $\alpha$ , p-JNK, p-ERK, and p-P38 in macrophages, thereby reducing the expression of related inflammatory cytokines. Moreover, Kin attenuated the infiltration of pro-inflammatory M1-type macrophages and articular cartilage degeneration, suggesting that targeting synovial macrophage polarization could be an effective strategy for treating OA. Further, Kin decreased macrophage CM and IL-1 $\beta$ -stimulated chondrocyte apoptosis. The schematic illustration shows the effects of Kin on the M1/M2 macrophage polarization and chondrocytes succinctly. All the results indicate that Kin could be an effective therapeutic candidate for OA treatment.

## Acknowledgements

This work was supported by the National Natural Science Foundation of China (No. 81672205), National Key R&D Programme (No. 2016YFC1102100, China) and the Shanghai Science and Technology Development Fund (Nos. 18DZ2291200 and 18441902700, China).

## Appendix A. Supporting information

Supporting data associated with this article can be found in the online version at doi:10.1016/j.apsb.2019.01.015.

## References

- Lawrence RC, Felson DT, Helmick CG, Arnold LM, Choi H, Deyo RA, et al. Estimates of the prevalence of arthritis and other rheumatic conditions in the United States. Part II. *Arthritis Rheum* 2008;**58**:26–35.
- Daugaard R, Tjur M, Slieden M, Lipperts M, Grimm B, Mechlenburg I. Are patients with knee osteoarthritis and patients with knee joint replacement as physically active as healthy persons?. *J Orthop Transl* 2018;**14**:8–15.
- Dieppe PA, Lohmander LS. Pathogenesis and management of pain in osteoarthritis. *Lancet* 2005;**365**:965–73.
- Kraus VB, Blanco FJ, Englund M, Karsdal MA, Lohmander LS. Call for standardized definitions of osteoarthritis and risk stratification for clinical trials and clinical use. *Osteoarthr Cartil* 2015;**23**:1233–41.
- Ettinger Jr. WH, Osteoarthritis II. pathology and pathogenesis. *Md State Med J* 1984;**33**:811–4.
- Boris Chan PM, Zhu L, Wen CY, Chiu KY. Subchondral bone proteomics in osteoarthritis: current status and perspectives. *J Orthop Transl* 2015;**3**:71–7.
- Bijlsma JW, Berenbaum F, Lafeber FP. Osteoarthritis: an update with relevance for clinical practice. *Lancet* 2011;**377**:2115–26.
- McAlindon TE, Bannuru RR, Sullivan MC, Arden NK, Berenbaum F, Bierma-Zeinstra SM, et al. OARSI guidelines for the non-surgical management of knee osteoarthritis. *Osteoarthr Cartil* 2014;**22**:363–88.
- Murray PJ, Wynn TA. Protective and pathogenic functions of macrophage subsets. *Nat Rev Immunol* 2011;**11**:723–37.
- Kamada N, Hisamatsu T, Okamoto S, Chinen H, Kobayashi T, Sato T, et al. Unique CD14 intestinal macrophages contribute to the pathogenesis of Crohn disease via IL-23/IFN- $\gamma$  axis. *J Clin Invest* 2008;**118**:2269–80.
- Han Q, Bing W, Di Y, Hua L, Shi-He L, Yu-Hua Z, et al. Kinsenoside screening with a microfluidic chip attenuates gouty arthritis through inactivating NF- $\kappa$ B signaling in macrophages and protecting endothelial cells. *Cell Death Dis* 2016;**7**:e2350.
- Guo Q, Wang Y, Xu D, Nossent J, Pavlos NJ, Xu J. Rheumatoid arthritis: pathological mechanisms and modern pharmacologic therapies. *Bone Res* 2018;**6**:15.
- Goodman SB, Qin L. Inflammation and the musculoskeletal system. *J Orthop Transl* 2017;**10**:A1–2.
- Gu Q, Yang H, Shi Q. Macrophages and bone inflammation. *J Orthop Transl* 2017;**10**:86–93.
- Huang R, Wang X, Zhou Y, Xiao Y. RANKL-induced M1 macrophages are involved in bone formation. *Bone Res* 2017;**5**:17019.
- Ley K. The second touch hypothesis: t cell activation, homing and polarization. *F1000Res* 2014;**3**:37.
- Stein M, Keshav S, Harris N, Gordon S. Interleukin 4 potently enhances murine macrophage mannose receptor activity: a marker of alternative immunologic macrophage activation. *J Exp Med* 1992;**176**:287–92.
- Doyle AG, Herbein G, Montaner LJ, Minty AJ, Caput D, Ferrara P, et al. Interleukin-13 alters the activation state of murine macrophages *in vitro*: comparison with interleukin-4 and interferon- $\gamma$ . *Eur J Immunol* 1994;**24**:1441–5.
- Davis MJ, Tsang TM, Qiu Y, Dayrit JK, Freij JB, Huffnagle GB, et al. Macrophage M1/M2 polarization dynamically adapts to changes in cytokine microenvironments in *Cryptococcus neoformans* infection. *MBio* 2013;**4**:e00264–13.
- Sun AR, Panchal SK, Friis T, Sekar S, Crawford R, Brown L, et al. Obesity-associated metabolic syndrome spontaneously induces infiltration of pro-inflammatory macrophage in synovium and promotes osteoarthritis. *PLoS One* 2017;**12**:e0183693.
- Wu JB, Chuang HR, Yang LC, Lin WC. A standardized aqueous extract of *Anoectochilus formosanus* ameliorated thioacetamide-induced liver fibrosis in mice: the role of Kupffer cells. *Biosci Biotechnol Biochem* 2010;**74**:781–7.
- Cui SC, Yu J, Zhang XH, Cheng MZ, Yang LW, Xu JY. Anti-hyperglycemic and antioxidant activity of water extract from *Anoectochilus roxburghii* in experimental diabetes. *Exp Toxicol Pathol* 2013;**65**:485–8.
- Tseng CC, Shang HF, Wang LF, Su B, Hsu CC, Kao HY, et al. Antitumor and immunostimulating effects of *Anoectochilus formosanus* Hayata. *Phytomedicine* 2006;**13**:366–70.
- Qu Y, Zhou L, Wang C. Effects of platycodin D on IL-1 $\beta$ -induced inflammatory response in human osteoarthritis chondrocytes. *Int Immunopharmacol* 2016;**40**:474–9.
- Lorenz J, Grassel S. Experimental osteoarthritis models in mice. *Methods Mol Biol* 2014;**1194**:401–19.
- Hayami T, Zhuo Y, Wesolowski GA, Pickarski M, Duong LT. Inhibition of cathepsin K reduces cartilage degeneration in the anterior cruciate ligament transection rabbit and murine models of osteoarthritis. *Bone* 2012;**50**:1250–9.
- Qiao H, Wang TY, Yu ZF, Han XG, Liu XQ, Wang YG, et al. Structural simulation of adenosine phosphate via plumbagin and zoledronic acid competitively targets JNK/Erk to synergistically attenuate osteoclastogenesis in a breast cancer model. *Cell Death Dis* 2016;**7**:e2094.
- Pritzker KP, Gay S, Jimenez SA, Ostergaard K, Pelletier JP, Revell PA, et al. Osteoarthritis cartilage histopathology: grading and staging. *Osteoarthr Cartil* 2006;**14**:13–29.

29. Krenn V, Morawietz L, Burmester GR, Kinne RW, Mueller-Ladner U, Muller B, et al. Synovitis score: discrimination between chronic low-grade and high-grade synovitis. *Histopathology* 2006;**49**:358–64.
30. Chawla A. Control of macrophage activation and function by PPARs. *Circ Res* 2010;**106**:1559–69.
31. Burr DB, Gallant MA. Bone remodelling in osteoarthritis. *Nat Rev Rheumatol* 2012;**8**:665–73.
32. Findlay DM, Kuliwaba JS. Bone-cartilage crosstalk: a conversation for understanding osteoarthritis. *Bone Res* 2016;**4**:16028.
33. Marijnissen AC, van Roermund PM, Verzijl N, Tekoppele JM, Bijlsma JW, Lafeber FP. Steady progression of osteoarthritic features in the canine groove model. *Osteoarthr Cartil* 2002;**10**:282–9.
34. Mastbergen SC, Marijnissen AC, Vianen ME, van Roermund PM, Bijlsma JW, Lafeber FP. The canine 'groove' model of osteoarthritis is more than simply the expression of surgically applied damage. *Osteoarthr Cartil* 2006;**14**:39–46.
35. Bellido M, Lugo L, Roman-Blas JA, Castaneda S, Caeiro JR, Dapia S, et al. Subchondral bone microstructural damage by increased remodeling aggravates experimental osteoarthritis preceded by osteoporosis. *Arthritis Res Ther* 2010;**12**:R152.
36. Hochberg MC, Altman RD, April KT, Benkhalti M, Guyatt G, McGowan J, et al. American College of Rheumatology 2012 recommendations for the use of nonpharmacologic and pharmacologic therapies in osteoarthritis of the hand, hip, and knee. *Arthritis Care Res (Hoboken)* 2012;**64**:465–74.
37. Hunter DJ. Pharmacologic therapy for osteoarthritis—the era of disease modification. *Nat Rev Rheumatol* 2011;**7**:13–22.
38. Kerschenmeyer A, Arlov O, Malheiro V, Steinwachs M, Rottmar M, Maniura-Weber K, et al. Anti-oxidant and immune-modulatory properties of sulfated alginate derivatives on human chondrocytes and macrophages. *Biomater Sci* 2017;**5**:1756–65.
39. Benito MJ, Veale DJ, FitzGerald O, van den Berg WB, Bresnihan B. Synovial tissue inflammation in early and late osteoarthritis. *Ann Rheum Dis* 2005;**64**:1263–7.
40. Bondeson J, Blom AB, Wainwright S, Hughes C, Caterson B, van den Berg WB. The role of synovial macrophages and macrophage-produced mediators in driving inflammatory and destructive responses in osteoarthritis. *Arthritis Rheum* 2010;**62**:647–57.
41. Kalkman HO, Feuerbach D. Antidepressant therapies inhibit inflammation and microglial M1-polarization. *Pharmacol Ther* 2016;**163**:82–93.
42. Tiemessen MM, Jagger AL, Evans HG, van Herwijnen MJ, John S, Taams LS. CD4<sup>+</sup>CD25<sup>+</sup>Foxp3<sup>+</sup> regulatory T cells induce alternative activation of human monocytes/macrophages. *Proc Natl Acad Sci U S A* 2007;**104**:19446–51.
43. Lawrence T, Natoli G. Transcriptional regulation of macrophage polarization: enabling diversity with identity. *Nat Rev Immunol* 2011;**11**:750–61.
44. Mancino A, Lawrence T. Nuclear factor- $\kappa$ B and tumor-associated macrophages. *Clin Cancer Res* 2010;**16**:784–9.
45. Hayden MS, Ghosh S. Shared principles in NF- $\kappa$ B signaling. *Cell* 2008;**132**:344–62.
46. Kim EK, Choi EJ. Compromised MAPK signaling in human diseases: an update. *Arch Toxicol* 2015;**89**:867–82.
47. Ghosh S, Karin M. Missing pieces in the NF- $\kappa$ B puzzle. *Cell* 2002;**109**Suppl:S81–96.
48. Zhou D, Huang C, Lin Z, Zhan S, Kong L, Fang C, et al. Macrophage polarization and function with emphasis on the evolving roles of coordinated regulation of cellular signaling pathways. *Cell Signal* 2014;**26**:192–7.
49. Xiang M, Liu T, Tan W, Ren H, Li H, Liu J, et al. Effects of kinsenoside, a potential immunosuppressive drug for autoimmune hepatitis, on dendritic cells/CD8<sup>+</sup> T cells communication in mice. *Hepatology* 2016;**64**:2135–50.
50. Hsiao HB, Hsieh CC, Wu JB, Lin H, Lin WC. Kinsenoside inhibits the inflammatory mediator release in a type-II collagen induced arthritis mouse model by regulating the T cells responses. *BMC Complement Altern Med* 2016;**16**:80.
51. Kobayashi M, Squires GR, Mousa A, Tanzer M, Zukor DJ, Antoniou J, et al. Role of interleukin-1 and tumor necrosis factor alpha in matrix degradation of human osteoarthritic cartilage. *Arthritis Rheum* 2005;**52**:128–35.
52. Goldring SR, Goldring MB. The role of cytokines in cartilage matrix degeneration in osteoarthritis. *Clin Orthop Relat Res* 2004:S27–36.
53. Kapoor M, Martel-Pelletier J, Lajeunesse D, Pelletier JP, Fahmi H. Role of proinflammatory cytokines in the pathophysiology of osteoarthritis. *Nat Rev Rheumatol* 2011;**7**:33–42.
54. Roman-Blas JA, Jimenez SA. NF- $\kappa$ B as a potential therapeutic target in osteoarthritis and rheumatoid arthritis. *Osteoarthr Cartil* 2006;**14**:839–48.
55. Cheon MS, Yoon T, Lee DY, Choi G, Moon BC, Lee AY, et al. *Chrysanthemum indicum* Linne extract inhibits the inflammatory response by suppressing NF- $\kappa$ B and MAPKs activation in lipopolysaccharide-induced RAW 264.7 macrophages. *J Ethnopharmacol* 2009;**122**:473–7.
56. Chen J, Fok KL, Chen H, Zhang XH, Xu WM, Chan HC. Cryptorchidism-induced CFTR down-regulation results in disruption of testicular tight junctions through up-regulation of NF- $\kappa$ B/COX-2/PGE2. *Hum Reprod* 2012;**27**:2585–97.